*International Journal of Modern Science and Technology* *Vol. 2, No. 1, 2017. Page 1-7.*
***http://www.ijmst.co/*** ***ISSN: 2456-0235.***

***Research Article***

# Pt–Ru–M/MWCNTs (M = Ni, Mo and Rh) Nano-catalysts for membraneless fuel cells: Effect of the pretreatment on the structural characteristics and perborate electro-oxidation

**K. Vijayaramalingam[1], S. Kiruthika[2], B. Muthukumaran[1,*]**

[1]Department of Chemistry, Presidency College, Chennai – 600 005, India.
[2]Department of Chemical Engineering, SRM University, Chennai – 603 203, India.

*Corresponding author's e-mail: dr.muthukumaran@yahoo.com

## Abstract

The synthesis, characterization and activity of Pd–Ir–M (M = Ni, Mo and Rh) electrocatalysts supported on multi-walled carbon nanotubes leading to enhancement of the electrocatalytic oxidation of sodium perborate is presented. The combination of monometallic Pd/MWCNTs, bimetallic Pd–Ir/MWCNTs and tri-metallic Pd–Ir–Ni/MWCNTs, Pd–Ir–Mo/MWCNTs and Pd–Ir–Rh/MWCNTs electrocatalysts were prepared by the ultrasonic-assisted chemical reduction method. Scanning electron microscopy (SEM), energy dispersive X-ray spectroscopy (EDX), transmission electron microscopy (TEM) and X-Ray diffraction (XRD) were used for the catalyst characterization. The synthesized electrocatalysts have been similar particle morphology and their particle sizes were 3-5 nm. The EDX results of the binary Pd–Ir/MWCNTs and the ternary Pd–Ir–Ni/MWCNTs, Pd–Ir–Mo/MWCNTs and Pd–Ir–Rh/MWCNTs catalysts were extremely close to the nominal values, indicating that the metals were loaded onto the carbon support without any obvious loss. The performances of the electrocatalysts have been examined in half-cell experiments using cyclic voltammetry (CV), CO stripping voltammetry and chronoamperometry (CA). The electrochemical results obtained at room temperature showed that the tri-metallic Pd–Ir–M (M = Ni, Mo and Rh) electrocatalysts displayed better catalytic activity toward sodium perborate oxidation compared to the other catalysts. In this study, the binary Pd−Ir/MWCNTs and ternary Pd−Ir−M/MWCNTs (M = Ni, Mo and Rh) anode catalysts were effectively tested by using single membraneless fuel cell using 0.15 M sodium perborate as the fuel and 0.1 M sodium perborate as the oxidant with 0.5 M $H_2SO_4$ as the electrolyte respectively. Based on the experimental results, we conclude that the Pd−Ir−Ni/MWCNTs demonstrate superior sodium perborate electro-oxidation than Pd−Ir−Mo/MWCNTs, Pd−Ir−Rh/MWCNTs, Pd−Ir/MWCNTs, Pd/MWCNTs.

**Keywords**: Multi-walled carbon nanotubes; Palladium; Iridium; Nickel; Membraneless sodium perborate fuel cell.

## Introduction

Recent reports have shown the increased attention of carbon nanotube (CNT) nanostructures, as they are the promising catalyst for fuel cells, hydrogen storage and many unique applications because of its electrochemical, electromagnetic and structural properties [1,2]. As the cost of the noble metals for the catalyst composition was relatively high, the loading were dropped to a level of < 1.0 mg/cm$^2$ [3]. Even though nanoparticle supporting strategy could dramatically reduce the Pd content in the catalysts, CO poisoning effect with which the active sites were deleteriously screened to suppress reaction kinetics and shorten the life time of the fuel cells [4]. To overcome the CO poisoning problem, a variety of binary, and ternary or quaternary alloy nanoparticles have been employed [5,6]. Unfortunately, it was highly challenging to load the metal alloy nanoparticles around CNTs homogeneously, and conventional impregnation methods have been suffered from the problems such as time consuming process and the easy catalyst contamination by side products [7]. Importantly, the preparation of binary or ternary metal electrocatalyst was much more challenging than that of pure ones because of the difficulty in uniform alloy formation and composition control.

*Received: 09.12.2016; Received after Revision: 05.01.2017; Accepted: 07.01.2017; Published: 12.01.2017*

In this regard, the effect of adding another component to Pd on the sodium perborate oxidation reaction has been intensively studied. Recent reports have shown an improved activity for various Pd–based catalysts, such as Pd–Co, Pd–Ni, Pd–Sn, Pd–Ru and Pd–Mo compositions [8-11]. Nevertheless, it is an ongoing task to improve the performance of anode catalysts to a level suitable for commercialization. A great attention has been compensated to Ni addition, which was low-cost and significantly to promote the sodium perborate oxidation on Pd. Recently; ternary electro-catalysts have been proved to be more active than their original mono- and bimetallic counterparts, as the adding together of a third component may alter the bifunctional, electronic or structural characteristics of the mono- and bimetallic catalyst surface [12,13]. With this regard, we synthesized a multi-walled carbon nanotubes supported ternary Pd–Ir–M (M = Ni, Mo and Rh) catalyst for the sodium perborate oxidation reaction. In this work we examined the effect of the addition of Ir, along with Ni, Mo and Rh to Pd on the sodium perborate oxidation in membraneless fuel cells.

## Materials and methods

### *Materials*

The metal precursors used for the preparation of electrocatalysts were adequate amounts of the $Pd(NO_3)_2{\cdot}2H_2O$, Aldrich Chem. Co., $IrCl_3$, Sigma Aldrich, $NiCl_2.6H_2O$, Sigma Aldrich, and $NaBO_3$ (from Riedel) reducing agent. Vulcan XC-72R carbon black (from Cabot Corp.,) was used as a support for the catalysts. Graphite plates (from E-TEK) were used as substrates for the catalyst to prepare the electrodes. Nafion® (DE 521, DuPont USA) dispersion was used to make the catalyst slurry. Sodium perborate (from Riedel) and $H_2SO_4$ (from Merck) were used as the fuel and as the electrolyte for electrochemical analysis respectively. All the chemicals were of analytical grade. Pt/MWCNTs (40% (w/w), from E-TEK) was used as the cathode catalyst.

### *Catalyst preparation*

Multi-walled Carbon nanotube supported ternary Pd–Ir–Ni nanoparticles were synthesized by ultrasonic assisted chemical reduction method. First, the required amounts of Vulcan XC-72R carbon black (from Cabot Corp.,) were ultrasonically dispersed in a mixture of ultrapure water (Millipore MilliQ, 18 MΩ cm) and then adequate amounts of the precursors were mixed with the solution. After mixing the solutions, the metal salts were reduced by $NaBH_4$. The synthesized materials were washed with distilled water and desiccated in a vacuum oven at 70°C. For comparison, the monometallic Pd/MWCNTs and bimetallic Pd–Ir/MWCNTs catalysts were prepared under the same conditions. The electrocatalytic mixtures and atomic ratios were Pd/MWCNTs (100), Pd–Ir/MWCNTs (60:40), Pd–Ir–Ni/MWCNTs (60:30:10), Pd–Ir–Mo/MWCNTs (60:30:10) and Pd–Ir–Rh/MWCNTs (60:30:10). The nominal loading of metals in the electrocatalysts was 40% and rest 60% (w/w) was carbon.

### *Physical characterization of the catalysts*

The morphology of the dispersed catalysts was examined using SEM (ZEISS EVO 50Scanning Electron Microscope) and TEM (Philips CM 12 Transmission) Electron Microscope). The particle size distribution and mean particle size were also evaluated using TEM. The crystal structure of the synthesized electrocatalysts were characterized by powder X-ray diffraction (XRD) using a Rigaku multiflex diffractometer (model RU-200 B) with Cu-$K_{\alpha1}$ radiation source ($\lambda_{K\alpha1}$ = 1.5406 $A^o$) operating at room temperature. The tube current was 40 mA with a tube voltage of 40 kV. The $2\theta$ angular regions between 20º and 90º were recorded at a scan rate of 5° $min^{-1}$. The mean particle size analyzed from TEM is verified by determining the crystallite size from XRD pattern using Scherrer formula. Pt (2 2 0) diffraction peak was selected to calculate crystallite size and lattice parameter of platinum. According to Scherrer's equation shown in Eq. (1).

$$d = \frac{0.9\lambda_{K\alpha1}}{ß_{2\theta}\cos\theta_{max}} \qquad (1)$$

where d is the average crystallite size, $\theta_{max}$ is the angle at the position of the peak maximum, $ß_{2\theta}$ is the width of the peak (in radians), 0.9 is the shape factor for spherical crystallite and $\lambda_{K\alpha1}$ is the wavelength of X-rays used. The lattice parameters of the catalysts were estimated according to Eq. (2).

$$a = \frac{\sqrt{2}\,\lambda_{K\alpha1}}{\sin\theta_{max}} \qquad (2)$$

 

where a, is the lattice parameter (nm) and all the other symbols have the same meanings as in Eq. 1. The atomic ratio of the catalysts was determined by an energy dispersive X-ray (EDX) analyzer, which was integrated with the TEM instrument.

### *Electrochemical measurements*

The electrochemical experiments were carried out in a conventional three-electrode cell at room temperature. Voltammetric curves using 0.5 M $H_2SO_4$ or 0.15 M sodium perborate/0.5 M $H_2SO_4$ electrolyte solutions purged with nitrogen gas were recorded with an electrochemical workstation (CHI-6650; CH Instruments, USA). Catalyst coated glassy-carbon electrode was used as the working electrode and a platinum wire was used as the counter electrode. Ag/AgCl in saturated KCl was used as the reference electrode. The activity of the electrocatalysts was determined by cyclic voltammetry in a half cell at a scan rate of 50 $mVs^{-1}$ between 0.05 and 1.2 V vs. Ag/AgCl and chronoamperometry (0.4 V vs. Ag/AgCl for 30 min).

## Result and discussions

### *Physical characterization*

*X-ray Diffraction analysis*

The structural information of the Pd–Ir–Ni/MWCNTs (60:30:10) catalyst was obtained by XRD and is shown in Fig. 1. The first peak located at the 2θ value of about 25° refers to the Vulcan XC-72R carbon black. The diffraction peaks at the 2θ values of 40.5°, 47.07°, 67.9°, and 81.90° are assigned to the (111), (200), (220) and (311) facets of the face-centered cubic (fcc) crystalline structure, respectively these four peaks were located at higher 2θ values with respect to that of pure Pd/MWCNTs, while at lower 2θ values with respect to that of bimetallic Pd–Ir (60:40) and trimetallic Pd–Ir–Ni/MWCNTs (60:30:10) catalysts and this can be attributed to the incorporation of a lower d space crystal structure of Ir than that of Pd suggesting the formation of Pd–Ir/MWCNTs alloy [14].

No significant shift is observed for Pd–Ni/MWCNTs catalysts, which suggests that Pd and Ni did not alloy well with this preparation method. The absence of peaks for either Ir or Ni or their oxides may be the reason for due to their poor crystallinity or low concentration. According to the Scherrer equation, the average crystallite size of the metal particles on the Pd–Ir–Ni/MWCNTs (60:30:10) catalyst is 4.9 nm. All the lattice parameters obtained from the XRD data are listed in Table 1. It should be noted that the change in the lattice parameters of all the alloy catalysts did not tremendous and this means the catalysts are not perfectly alloyed. However the small differences in lattice constant may suggest a prominent role of the electrocatalysts for their enhancement in catalytic activity.

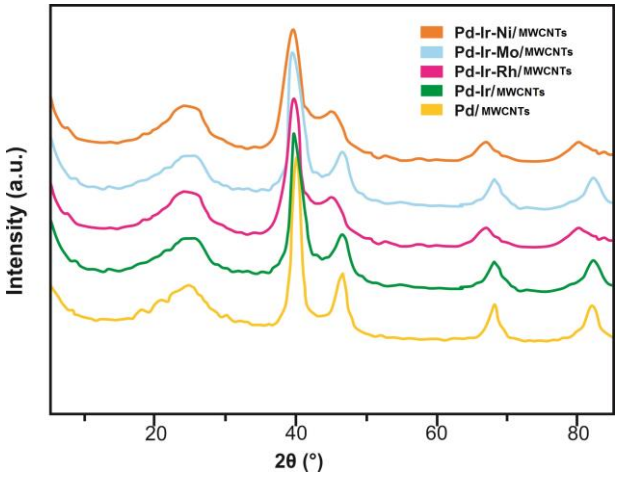


Fig. 1. X-ray diffraction patterns of Pd–Ir–Ni/MWCNTs, Pd–Ir–Mo/MWCNTs, Pd–Ir–Rh/MWCNTs, Pd–Ir/MWCNTs and Pd/MWCNTs electrocatalysts

Table 1. The EDX composition, XRD and TEM particle size obtained for different atomic ratios of electrocatalysts

| Electrocatalyst | Nominal atomic ratio | | | EDX atomic Ratio | | | Lattice parameter (nm) | Crystallite size (nm) | Particle size from TEM (nm) |
|---|---|---|---|---|---|---|---|---|---|
| | Pd | Ir | M* | Pd | Ir | M | | | |
| Pd/MWCNTs | 100 | - | - | 99 | - | - | 0.3894 | 5.6 | 5.4 |
| Pd–Ir/MWCNTs | 60 | 40 | - | 58 | 42 | - | 0.3889 | 5.4 | 5.3 |
| Pd–Ir–Rh/MWCNTs | 60 | 30 | 10 | 62 | 29 | 09 | 0.3886 | 5.3 | 5.2 |
| Pd–Ir–Mo/MWCNTs | 60 | 30 | 10 | 61 | 31 | 08 | 0.3885 | 5.1 | 5.0 |
| Pd–Ir–Ni/MWCNTs | 60 | 30 | 10 | 62 | 29 | 09 | 0.3883 | 5.0 | 4.9 |

(*M = Rh, Mo and Ni)

 

*Transmission Electron Microscopy analysis*

Fig. 2 shows the TEM image and histogram of the metal particle size have been distributed of the Pd–Ir–Ni/MWCNTs (60:30:10) catalyst. It can be observed that the metal particles on the Pd–Ir–Ni/MWCNTs catalyst exhibit a spherical shape and these were well dispersed on the carbon powder support without severe aggregation. The metal particle size distribution of the Pd–Ir–Ni/MWCNTs catalyst was evaluated from an ensemble of 200 particles. Based on this evaluation, the Pd–Ir–Ni/MWCNTs catalyst shows a metal particle size distribution ranging from 1.5 to 7 nm and the average metal particle size is 4.9 nm, which is almost the same as the value predicted from the XRD data.

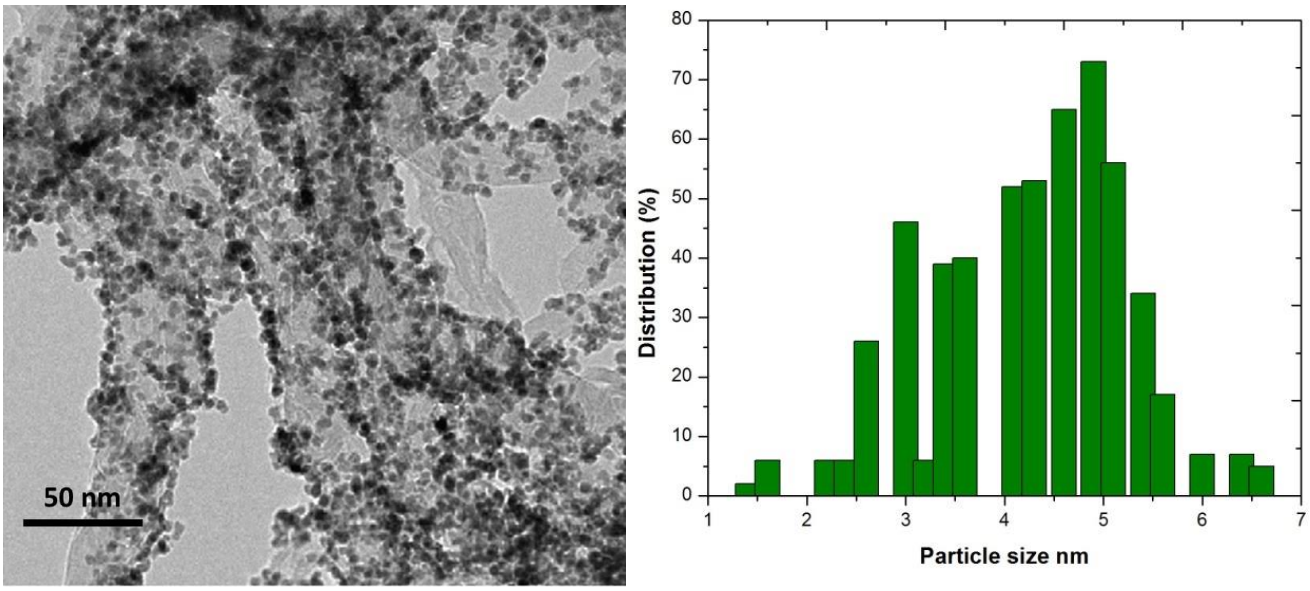


Fig. 2. TEM image and histogram of Pd–Ir–Ni/MWCNTs catalysts

*Energy Dispersive X-ray Spectroscopy analysis*

The composition of carbon-supported Pd–Ir–Ni electrocatalysts was determined by EDX analysis and the corresponding results are shown in Fig. 3. It was found that EDX composition of the prepared catalyst is close to the nominal values which indicate the presence of Pd, Ir and Ni along with carbon.

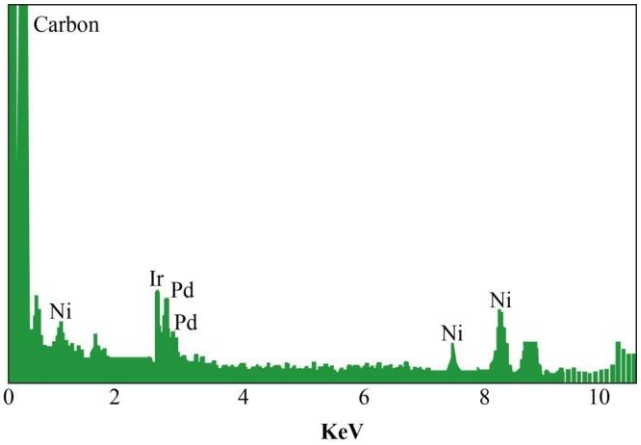


Fig. 3. EDX spectra of Pd–Ir–Ni/MWCNTs catalysts

***Electrochemical Characterization***

*Cyclic Voltammetry*

Fig. 4a presents the cyclic voltammograms of 0.5M $H_2SO_4$ solution at the different catalyst electrodes. The charge–discharge current of the double layer at the Pd–Ir–Ni/MWCNTs catalyst electrode is largest among all the catalyst electrodes because as mentioned above, the Pd–Ir–Ni/MWCNTs catalyst possesses the smallest average size of the metal particles and it was one of the largest surface area among all the catalysts. Hence Pd–Ir–Ni/MWCNTs catalyst possesses the excellent ability whereasPd–Ir/MWCNTs and Pd/MWCNTs has the poor ability for the adsorption/desorption of hydrogen, and the current densities of the adsorption/desorption peak of hydrogen around 0V are decreased according to the order of the Pd–Ir–Ni/MWCNTs> Pd–Ir–Mo/MWCNTs> Pd–Ir–Rh/MWCNTs> Pd–Ir/MWCNTs> Pd/MWCNTs catalysts. These results are similar to the results of observed and calculated from XRD data.

The catalytic activity of cyclic voltammetry for sodium perborate electro-

 

oxidation of Pd/MWCNTs (100), Pd–Ir/MWCNTs (60:40), Pd–Ir–Ni/MWCNTs (60:30:10), Pd–Ir–Mo/MWCNTs (60:30:10) and Pd–Ir–Rh/MWCNTs (60:30:10) electrocatalysts in 0.5M $H_2SO_4$ with 0.15 M sodium perboratesolution in the potential range of -0.2 V to 0.8 V vs. Ag/AgCl were shown in Fig. 4b and they are all characterized by two well-defined peaks, the one is anodic sweep curve and the other one is cathodic sweep curve.

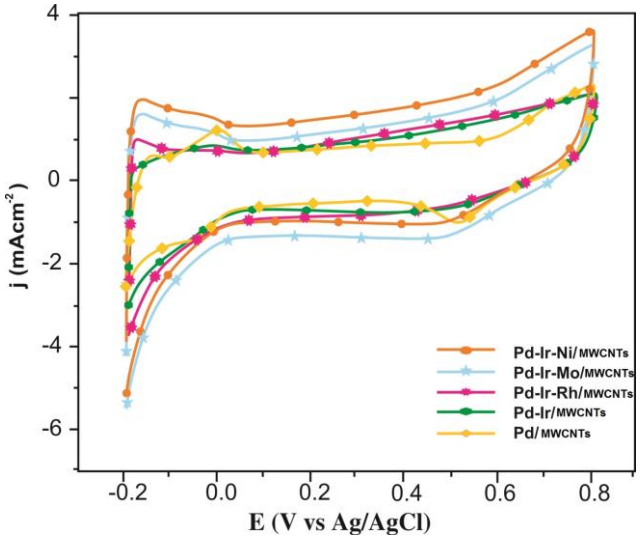


Fig. 4a. Cyclic voltammograms of Pd–Ir–Ni/MWCNTs (60:30:10),Pd–Ir–Mo/MWCNTs (60:30:10),Pd–Ir–Rh/MWCNTs (60:30:10), Pd–Ir/MWCNTs (60:40) and Pd/MWCNTs (100) catalysts in 0.5M $H_2SO_4$

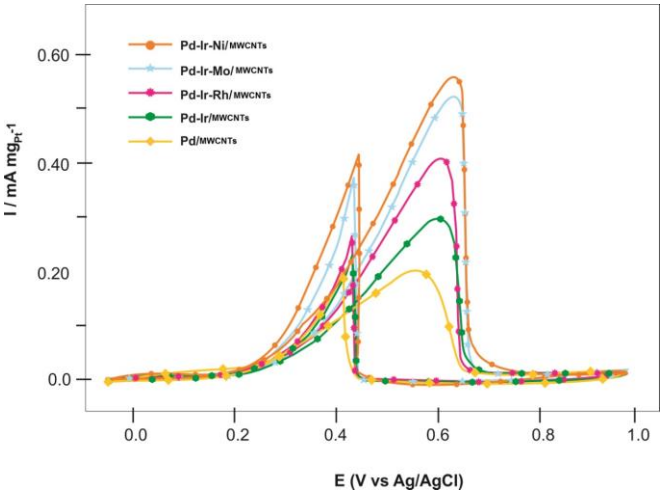


Fig. 4b. Cyclic voltammetry of Pd/MWCNTs (100), Pd–Ir/MWCNTs (60:40), Pd–Ir–Ni/MWCNTs (60:30:10), Pd–Ir–Mo/MWCNTs (60:30:10) and Pd–Ir–Rh/MWCNTs (60:30:10) electrocatalysts

The Pd–Ir–Ni/MWCNTs (60:30:10) exhibited the highest catalytic activity. For comparison, the catalytic activity of Pd/MWCNTs (100), Pd–Ir/MWCNTs (60:40), Pd–Ir–Mo/MWCNTs (60:30:10) and Pd–Ir–Rh/MWCNTs (60:30:10) catalysts were tested. The onset potential of sodium perborate oxidation for Pd–Ir–Ni/MWCNTs (60:30:10) catalyst is less negative than those of Pd–Ir–Mo/MWCNTs, Pd–Ir–Rh/MWCNTs, Pd–Ir/MWCNTs and Pd/MWCNTs catalysts, indicating good electrocatalytic activity as shown in Table 2.

Table 2 CV results of Pd/MWCNTs (100), Pd–Ir/MWCNTs (60:40), Pd-Ir-Rh/MWCNTs (60:30:10), Pd-Ir-Mo/MWCNTs (60:30:10) and Pd–Ir–Ni/MWCNTs (60:30:10) electrocatalysts

| Catalysts | Scan rate 50 $mVs^{-1}$ | |
|---|---|---|
| | Positive peak potential (V vs. Ag/AgCl) | Peak current density ($mA/cm^2$) |
| Pd/MWCNTs (100) | 0.513 | 19.3 |
| Pd–Ir/MWCNTs (60:40) | 0.585 | 29.9 |
| Pd–Ir–Rh/MWCNTs (60:30:10) | 0.589 | 40.1 |
| Pd–Ir-Mo/MWCNTs (60:30:10) | 0.598 | 52.3 |
| Pd–Ir-Ni/MWCNTs (60:30:10) | 0.605 | 55.6 |

The onset potential of sodium perborate on Pd–Ir–Ni/MWCNTs (60:30:10) is at 0.605 V which is a factor of 0.1 V negative than that of the Pd/MWCNTs (100) catalysts. The Pd–Ir–Ni/MWCNTs (60:30:10) shows highest peak current density at 0.605 V peak potential. Hence possesses highest catalytic activity towards sodium perborate oxidation than Pd–Ir-Mo/MWCNTs (60:30:10), Pd–Ir-Rh/MWCNTs (60:30:10), Pd–Ir/MWCNTs (60:40) and Pd/MWCNTs (100) catalysts indicating that Pd–Ir–Ni/MWCNTs (60:30:10) is a promising catalyst for sodium perborate electro-oxidation.

*Chronoamperometry*

Fig. 5 shows the long-term reactivity of sodium perborate oxidation on Pd–Ir–Ni/MWCNTs (60:30:10), Pd–Ir–Mo/MWCNTs (60:30:10), Pd–Ir–Rh/MWCNTs (60:30:10), Pd–Ir/MWCNTs (60:40) and Pd/MWCNTs (100) catalysts have been investigated by chronoamperometry (CA) in a 0.15 M sodium perborate + 0.5M $H_2SO_4$solution with an applied potential of 0.1 V vs. Ag/AgCl. The durability test was taken for about 3000s. The results clearly show a strong correlation between Pd–Ir–

 

Ni/MWCNTscontacts and long-term sodium perborate oxidation reaction.

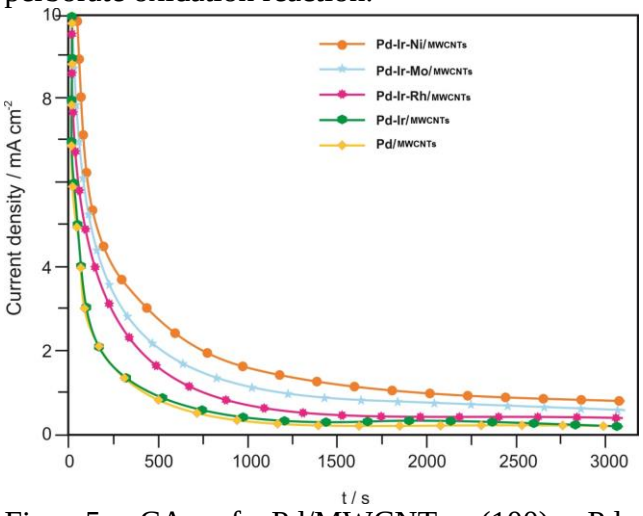


Fig. 5. CA of Pd/MWCNTs (100), Pd–Ir/MWCNTs (60:40), Pd–Ir–Ni/MWCNTs (60:30:10), Pd–Ir–Mo/MWCNTs (60:30:10) and Pd–Ir–Rh/MWCNTs (60:30:10) electrocatalysts

During the experiment, there was a sharp decrease in the current density and after 120 s, it becomes relatively stable. This behavior can be explained by assuming that initially the active sites were free from adsorbed sodium perborate molecules, but a new adsorption of sodium perborate molecules is a function of the liberation of the active sites by sodium perborate oxidation. The ternary Pd–Ir–Ni/MWCNTs (60:30:10) electrocatalysts gave higher current than the other electrocatalysts. This is attributed to the change of electronic structure induced by ternary Pd–Ir–Ni/MWCNTs (60:30:10) electrocatalysts.

*Single Cell Performance Test*

The microfluidic construction of laminar flow-based membraneless fuel cells overcomes the fuel crossover and water management issues that the plague membrane-based fuel cells (i.e., PEMFC, DMFC) and enables independent control of stream characteristics (i.e., flow-rate and composition). Here we concentrated on maximizing cell performance, in terms of power density, by tailoring various structural characteristics and catalytic activity of carbon supported ternary Pd–Ir–Ni catalysts. The electrocatalysts Pd–Ir–Ni/MWCNTs (60:30:10), Pd–Ir–Mo/MWCNTs (60:30:10), Pd–Ir–Rh/MWCNTs (60:30:10), Pd–Ir/MWCNTs (60:40) and Pd/MWCNTs (100) evaluated as anode catalysts for sodium perborate electro-oxidation were shown in Fig. 6.

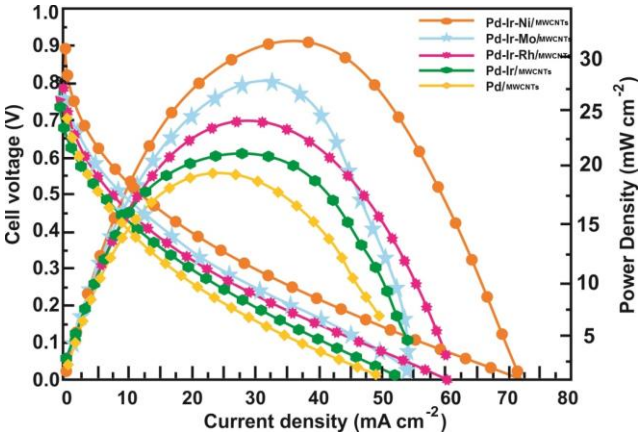


Fig. 6. Polarization and power density curves of different catalyst at 2 mg $cm^{-2}$ catalyst loading on anode and cathode

The ternary Pd–Ir–Ni/MWCNTs (60:30:10) anode catalysts shows maximum catalytic activity towards sodium perborate electro-oxidation than the other electrocatalysts tested. It was observed that the cell performance of the ternary Pd–Ir–Ni/MWCNTs (60:30:10) electrocatalyst was better than the other catalysts with a peak power density value of 34.93 $mWcm^{-2}$. The addition of Ni into Pd–Ir/MWCNTs results in the rises in the cell performances of single membraneless sodium perborate fuel cell test.The current densities for Pd–Ir–Ni/MWCNTs (60:30:10), Pd–Ir-Mo/MWCNTs (60:30:10), Pd–Ir-Rh/MWCNTs (60:30:10), Pd–Ir/MWCNTs (60:40), and Pd/MWCNTs (100) were 75.56, 72.42, 63.5, 56.62 and 50.1 $mAcm^{-2}$ respectively. The enhanced catalytic performance of Pd–Ir–Ni/MWCNTs (60:30:10) may be attributed to its special composition and surface electronic state in electro-oxidation of sodium perborate.

## Conclusions

In conclusion, the Pd–Ir–Ni/MWCNTs (60:30:10) electrocatalyst with a small average size and low relative crystallinity of the Pd–Ir particles can be prepared by ultrasonic assisted chemical reduction method at room temperature. When the atomic ratio of Pd, Ir and Ni is suitable theelectrocatalytic activity of the Pd–Ir–Ni/MWCNTs catalyst for the oxidation of sodium perborate is much better than that of the Pd/MWCNTs catalyst. The onset potential of the anodic peak of sodium perborate at the Pd–Ir–Ni/MWCNTs catalyst is lower than that of the Pd–Ir–Mo/MWCNTs, Pd–Ir–Rh/MWCNTs, Pd–Ir/MWCNTs and Pd/MWCNTs catalyst and the peak current density at the Pd–Ir–Ni/MWCNTs

 

catalyst is much higher than that at the Pd/MWCNTs catalyst. This is attributed to that Ir can stimulate the oxidation of sodium perborate at Pd–Ni/MWCNTs through the direct pathway. However, when the content of Ir in the Pd–Ir–Ni/MWCNTs catalyst is too high the electrocatalytic activity of the Pd–Ir–Ni/MWCNTs catalyst would be decreased. It was worth mentioning that these catalysts were less expensive compared to the commercial electrocatalysts

## Conflict of interest

Authors declare there are no conflicts of interest.

## References

[1] Mahendran S, Anbuselvan C. Kinetics and mechanism of oxidation of 5-(4'-bromophenyl)-5-oxopentanoicacid by acid permanganate. International Journal of Modern Science and Technology. 2016;1:106–110.

[2] Priya M, Elumalai M, Kiruthika S and Muthukumaran B. Influences of supporting materials for Pt-Ru binary catalyst in Ethanol fuel cell. International Journal of Modern Science and Technology. 2016;1:5–11.

[3] Georgakilas V, Gournis D, Tzitzios V, Pasquato L, Guldi DM, Prato M. Decorating carbon nanotubes with metals or semiconductor nanoparticles. J Mater Chem. 2007;17:2679–2694.

[4] Lamy C, Lima A, Le Rhun V, Delime F, Coutanceau C, Leger JM. Recent advances in the development of direct alcohol fuel cells (DAFC). J Power Sources. 2002;105:283–96.

[5] Bagchi J, Bhattacharya SK. Properties of anodic RuNiOx (OH)y catalysts synthesized on carbon supports with various dispersion degree. Trans Metal Chemistry. 2007;32:47–55.

[6] He Q, Chen W, Chen S, Laufek F, Mukerjee S. Carbon-supported PdM (M= Au and Sn) nanocatalysts for the electrooxidation of ethanol in high pH media. J Power Sources. 2009;187:298–304.

[7] Ksar F, Ramos L, Keita B, Nadjo L, Beaunier P, Remita H. Bimetallic palladium−gold nanostructures: application in ethanol oxidation. Chem Mater. 2009;21:3677–3683.

[8] Li X, Huang Q, Zou Z, Xia B, Yang H. Low temperature preparation of carbon-supported Pd Co alloy electrocatalysts for methanol-tolerant oxygen reduction reaction. Electrochim Acta. 2008;52:6662–6667.

[9] Liao S, Holmes KA, Tsaprailis H, Birss VI. High performance PtRuIr catalysts supported on carbon nanotubes for the anodic oxidation of methanol. J Am Chem Soc. 2006;128:3504–3505.

[10] Qiu CC, Shang R, Xie YF, Bu YR, Li CY, Ma HY. Electrocatalytic activity of bimetallic Pd–Ni thin films towards the oxidation of methanol and ethanol. Mater Chem Phys. 2010;120:323–330.

[11] Sanchez GR, Madeira HY, Feria OS. PdNi electrocatalyst for oxygen reduction in acid media. Int J Hydrogen Energy. 2008;33:3596–3600.

[12] Sarkar A, Murugan AV, Manthiram A. Synthesis and characterization of nanostructured Pd− Mo electrocatalysts for oxygen reduction reaction in fuel cells. J Phys Chem C. 2008;112:12037–12043.

[13] Kalaikathir SPR, Begila David S. Synthesis and characterization of nanostructured carbon-supported Pt electrocatalysts for membraneless methanol fuel cells. International Journal of Modern Science and Technology. 2016;1:199–212.

[14] Vijayaramalingam K, Kiruthika S, Muthukumaran B. Promoting Effect of Third Metal (M = Ni, Mo and Rh) on Pd–Ir Binary Alloy Catalysts in Membraneless Sodium Perborate Fuel Cells. International Journal of Modern Science and Technology. 2016;1:257–263.

*******

 